Polymer 51 (2010) 6123–6131

Contents lists available at ScienceDirect

Polymer

journal homepage: www.elsevier.com/locate/polymer

Donor–acceptor–donor type conjugated polymers for electrochromic applications: benzimidazole as the acceptor unit

Hava Akpınar [a], Abidin Balan [a], Derya Baran [a], Elif Köse Ünver [a], Levent Toppare [a,b,c,*]

[a] *Department of Chemistry, Middle East Technical University, 06531 Ankara, Turkey*
[b] *Department of Biotechnology, Middle East Technical University, 06531 Ankara, Turkey*
[c] *Department of Polymer Science and Technology, Middle East Technical University, 06531 Ankara, Turkey*

ARTICLE INFO

Article history:
Received 28 July 2010
Received in revised form
17 October 2010
Accepted 22 October 2010
Available online 30 October 2010

Keywords:
Benzimidazole
Donor-acceptor approach
Electrochromism

ABSTRACT

Donor–acceptor–donor (DAD) type benzimidazole (BIm) and 3,4 ethylenedioxythiophene (EDOT) bearing monomers were synthesized and electrochemically polymerized. Pendant group at 2-C position of the imidazole ring was functionalized with phenyl (P1), EDOT (P2) and ferrocene (P3) in order to observe substituent effect on electrochemical and electrochromic properties of corresponding polymers. Spectroelectrochemical results showed that different pendant groups resulted in polymers with slightly different optical band gaps (1.75, 1.69 and 1.77 eV respectively) and different number of achievable colored states. Optoelectronic performance and comparison of results with other well known π-accepting benzazole bearing DAD type polymers were reported in detail.

1. Introduction

Electrically conducting, conjugated polymers (CPs) have been attracting great deal of interest due to their suitability for numerous applications including photovoltaics (PVs) [1], field effect transistors (FETs) [2], light emitting diodes (LEDs) [3] and electrochromic devices (ECDs) [4]. The use of CPs as materials which possess the ability to change color reversibly by altering redox state has a fast receiving attention. Synthetic availability of conducting polymers allows fine tuning in electronic and optical properties [5]. The great majority of CPs are colored in their neutral states since the energy difference between their HOMO and LUMO levels, termed as band gap (E_g), lies within the visible region. Through charge carrier formation on polymer backbone upon oxidation, the intensity of the $\pi-\pi^*$ transition decreases, and low-energy transitions emerge to produce a second colored or a transmissive state. By all means, band gap energy of these polymers is dominant among factors affecting optical and electronic properties [6]. There are plenty of synthetic routes for adjusting the band gap however, donor–acceptor–donor (DAD) method can be considered as the most utilized one among all [7].

The DA type polymers consisting of alternating electron donors and acceptors generally have lower band gaps and wider bandwidths than either of the corresponding homo-polymers when D and A moieties match appropriately [8]. The basic idea here is the contributions of donor and acceptor heterocycles to HOMO and LUMO energy levels of the polymer [9]. Thus, mainly the polymer is expected to have an ionization potential (IP) closer to the donor and an electron affinity (EA) closer to the acceptor [10]. DAD type polymers thus, can be classified as copolymers made up with donor and acceptor units and match between these units designate the resulting polymer's properties. Comprehensive reports of Yamamoto et al. on n-type π-conjugated units, benzimidazole (BIm), benzothiadiazole (BTd), benzotriazole (BTz) and benzoselenadiazole (BSe) which are potentially acceptor units, showed that their electrochemical and optical characteristics are slightly different since they possess different atoms on their isoelectronic structures [11]. These heterocyclic benzazole derivatives exhibit high electron transporting ability because of the electron withdrawing imine (C=N) bonds on their backbones.

Previously reported DAD type polymers obtained by coupling benzazoles with electron donating EDOT resulted in fine tuned electrochromic properties. BTd derivative DAD polymer was synthesized [12] and later it was shown to be the first green to transmissive electrochromic polymer [13]. BSe based polymer was

---

[*] Corresponding author. Middle East Technical University Department of Chemistry, Department of Biotechnology, Department of Polymer Science and Technology, Turkey. Tel.: +90 312 2103251; fax: +90 312 2101280.
E-mail address: toppare@metu.edu.tr (L. Toppare).

0032-3861/$ – see front matter © 2010 Elsevier Ltd. All rights reserved.
doi:10.1016/j.polymer.2010.10.045

also investigated as a green to transmissive polymer with red shifted absorptions compared to BTd derivative [14]. Recently, introduction of BTz units on PEDOT resulted in the enhancement of electrochromic properties such as optical contrast, switching time and coloration efficiency compare to parent polymer PEDOT [15]. Although, BTd, BSe and BTz based polymers and their different copolymers have been studied extensively in literature, DAD type electrochromic polymers with BIm as the acceptor unit are still unexplored up to date. Instead, benzimidazoles which are an important molecule in vitamin B12 have been widely used in biological applications. It was shown that they have antibacterial, virucidal and antitumor properties [16]. Polybenzimidazoles on the other hand showed great thermal stability and resistance to high temperatures [17].

In this report, we highlight the synthesis and optoelectronic properties of BIm based DAD type polymers containing EDOT as the donor unit. Substituent effect on electrochemical and optical properties was investigated. Substitution of benzene and EDOT units on 2-C position of BIm resulted in two homologue polymers. Additionally, ferrocene (Fc) incorporation as pendant group was expected to reveal different redox behaviors due to its reversible and well defined electrochemical signal. Electrochromic properties of polymers were also compared with their different acceptor unit analogues where EDOT is the donor unit, to have a better understanding on acceptor unit effect.

2. Experimental section

2.1. General

All chemicals were purchased from commercial sources and used without further purification. All reactions were carried out under argon atmosphere unless otherwise mentioned. 4,7-Dibromobenzothiadiazole [18], 3,6-dibromobenzene-1,2-diamine [19], tributyl(2,3-dihydrothieno[3,4-*b*][1,4]dioxin-7-yl)stannane [20], 2,3-dihydrothieno[3,4-*b*][1,4]dioxine-5-carbaldehyde [7], 4,7-dibromo-2-phenyl-1*H*-benzo[d]imidazole [11a] and 4,7-dibromo-2-(2,3-dihydrothieno[3,4-*b*][1,4]dioxin-5-yl)-1*H*-benzo[d]imidazole [11a] were synthesized according to previously published procedures. Electrochemical studies were performed in a three-electrode cell consisting of an Indium Tin Oxide doped glass slide (ITO) as the working electrode, platinum wire as the counter electrode, and Ag wire as the pseudo reference electrode under ambient conditions using a Voltalab 50 potentiostat. ^{1}H and ^{13}C NMR spectra were recorded in CDCl$_3$ on Bruker Spectrospin Avance DPX-400 Spectrometer. Chemical shifts were given in ppm downfield from tetramethylsilane. Varian Cary 5000 UV–Vis spectrophotometer was used to perform the spectroelectrochemical studies of polymers. Mass analysis was carried out on a Bruker time-of flight (TOF) mass spectrometer with an electron impact ionization source.

2.2. Synthesis

*2.2.1. 4,7-Dibromo-2-ferrocenyl-1H-benzo[d]imidazole (**3c**)*

3,6-Dibromobenzene-1,2-diamine (500 mg, 1.88 mmol) and ferrocenecarboxaldehyde (483 mg, 2.41 mmol) were dissolved in 30 ml methanol (MeOH). After clear solution was obtained, 20 mg iodine were added to the mixture and stirred at room temperature overnight. Subsequent precipitate was filtered and washed with cold MeOH (3×50 ml). The product was obtained as orange solid (530 mg, yield: 77%) after re-crystallization in MeOH. ^{1}H (400 MHz, DMSO-d$_6$, δ): 12.80 (s, 1H), 7.30 (m, 2H), 5.26 (t, 2H), 4.53 (t, 2H), 4.15 (s, 5H). ^{13}C NMR (100 MHz, DMSO-d$_6$, δ): 155.4, 142.9, 134.8, 133.3, 132.1, 125.4, 125.3, 110.1, 105.6, 101.7, 101.6, 99.5, 79.1, 72.8, 70.3, 69.5, 68.0.

*2.2.2. 4-(2,3-Dihydrothieno[3,4-b][1,4]dioxin-5-yl)-7-(2,3-dihydrothieno[3,4-b][1,4]dioxin-7-yl)-2-benzyl-1H-benzo[d]imidazole (**M1**)*

In a three necked round-bottom flask fitted with a condenser and argon inlet, 4,7-dibromo-2-phenyl-1*H*-benzo[d]imidazole (100 mg, 0.28 mmol) and tributyl(2,3-dihydrothieno[3,4-*b*][1,4]dioxin-7-yl)stannane (490 mg, 1.14 mmol) were dissolved in 25 ml of dry THF. After 30 min stirring under argon flow, dichlorobis(triphenyl phosphine)palladium(II) (30 mg, 0.027 mmol) was added at room temperature. The mixture was left to reflux for 18 h. Solvent was evaporated under vacuum and the crude product was purified by column chromatography over silica gel 1:2 (ethylacetate:hexane) to obtain M1 as yellow solid (78 mg, yield: 58.7%). ^{1}H (400 MHz, CDCl$_3$, δ): 10.61 (s, 1H), 8.09 (d, 2H), 8.05 (d, 1H), 7.50 (m, 3H), 7.42 (d, 1H), 6.52 (s, 1H), 6.44 (s, 1H), 4.48 (d, 2H), 4.38 (d, 4H), 4.29 (d, 2H). ^{13}C NMR (100 MHz, CDCl$_3$, δ): 150.4, 142.0, 141.5, 141.1, 139.5, 135.9, 131.5, 130.2, 129.9, 129.0, 128.2, 126.4, 125.3, 123.9, 121.3, 120.7, 116.7, 114.6, 114.5, 100.9, 99.2, 65.6, 64.9, 64.5, 64.4. MS (*m*/*z*): 475 [M^{+}].

*2.2.3. 2,4-Bis(2,3-dihydrothieno[3,4-b][1,4]dioxin-5-yl)-7-(2,3-dihydrothieno[3,4-b][1,4]dioxin-7-yl)-1H-benzo[d]imidazole (**M2**)*

This monomer was prepared with the same procedure described for **M1** using 4,7-dibromo-2-(2,3-dihydrothieno[3,4-*b*][1,4]dioxin-5-yl)-1*H*-benzo[d]imidazole (200 mg, 0.48 mmol), tributyl(2,3-dihydrothieno[3,4-*b*][1,4]dioxin-7-yl)stannane (829.1 mg, 1.92 mmol), and dichlorobis(triphenyl phosphine) palladium(II) (50 mg, 0.045 mmol) in 35 ml of dry THF. After removing the solvent on rotary evaporator, the residue was subjected to column chromatography on silica gel, eluting with 1:1 (ethyl acetate:hexane) to obtain **M2** as yellow solid (156 mg, yield: 60.3%). ^{1}H (400 MHz, CDCl$_3$, δ): 10.86 (s, 1H), 8.02 (d, 1H), 7.38 (d, 1H), 6.50 (s, 1H), 6.49 (s, 1H), 6.43 (s, 1H), 4.36 (m, 12H). ^{13}C NMR (100 MHz, CDCl$_3$, δ): 145.2, 143.9, 140.9, 140.3, 139.7, 139.2, 135.5, 129.1, 127.3, 124.6, 120.5, 119.7, 114.9, 114.1, 110.3, 107.9, 101.9, 101.3, 98.7, 64.7, 64.6, 64.3, 63.3, 63.2. MS (*m*/*z*): 539 [M^{+}].

*2.2.4. 4-(2,3-Dihydrothieno[3,4-b][1,4]dioxin-5-yl)-7-(2,3-dihydrothieno[3,4-b][1,4]dioxin-7-yl)-2-ferrocenyl-1H-benzo[d]imidazole (**M3**)*

This compound was also prepared with the same procedure described above, using 4,7-dibromo-2-ferrocenyl-1*H*-benzo[d]imidazole (500 mg, 1.08 mmol), tributyl(2,3-dihydrothieno[3,4-*b*][1,4]dioxin-7-yl)stannane (829.1 mg, 1.92 mmol), and dichlorobis(triphenyl phosphine)palladium(II) (70 mg, 0.064 mmol) in 50 ml of dry THF. In this case completion of the reaction was achieved by an additional 30 h of reflux as monitored by TLC. Solvent was removed under vacuum and the crude product was purified by column chromatography over silica gel 1:3 (ethylacetate:hexane) to obtain **M3** as orange solid (430 mg, yield: 68%). ^{1}H (400 MHz, DMSO-d$_6$, δ): 11.69 (s, 1H), 7.92 (d, 1H), 7.09 (d, 1H), 6.75 (s, 1H), 6.69 (s, 1H), 5.22 (t, 2H), 4.48 (t, 2H), 4.39 (m, 4H), 4.28 (m, 4H), 4.14 (s, 5H). ^{13}C NMR (100 MHz, DMSO-d$_6$, δ): 152.7, 142.2, 141.3, 140.1, 139.1, 138.4, 132.4, 124.3, 122.0, 121.5, 119.1, 113.8, 112.6, 100.7, 98.8, 79.3, 79.1, 78.9, 78.6, 74.2, 69.8, 69.4, 67.9, 67.8, 64.8, 64.6, 64.2, 64.0, 56.0. MS (*m*/*z*): 583 [M^{+}].

3. Results and discussions

3.1. Synthesis

Synthesis of electroactive donor–acceptor–donor (DAD) type monomers was achieved as shown in Scheme 1. Bromination of benzothiadiazole was performed with Br$_2$ in HBr to give the 4,7-dibromobenzothiadiazole (**2**) in very high yields (98%) [18].

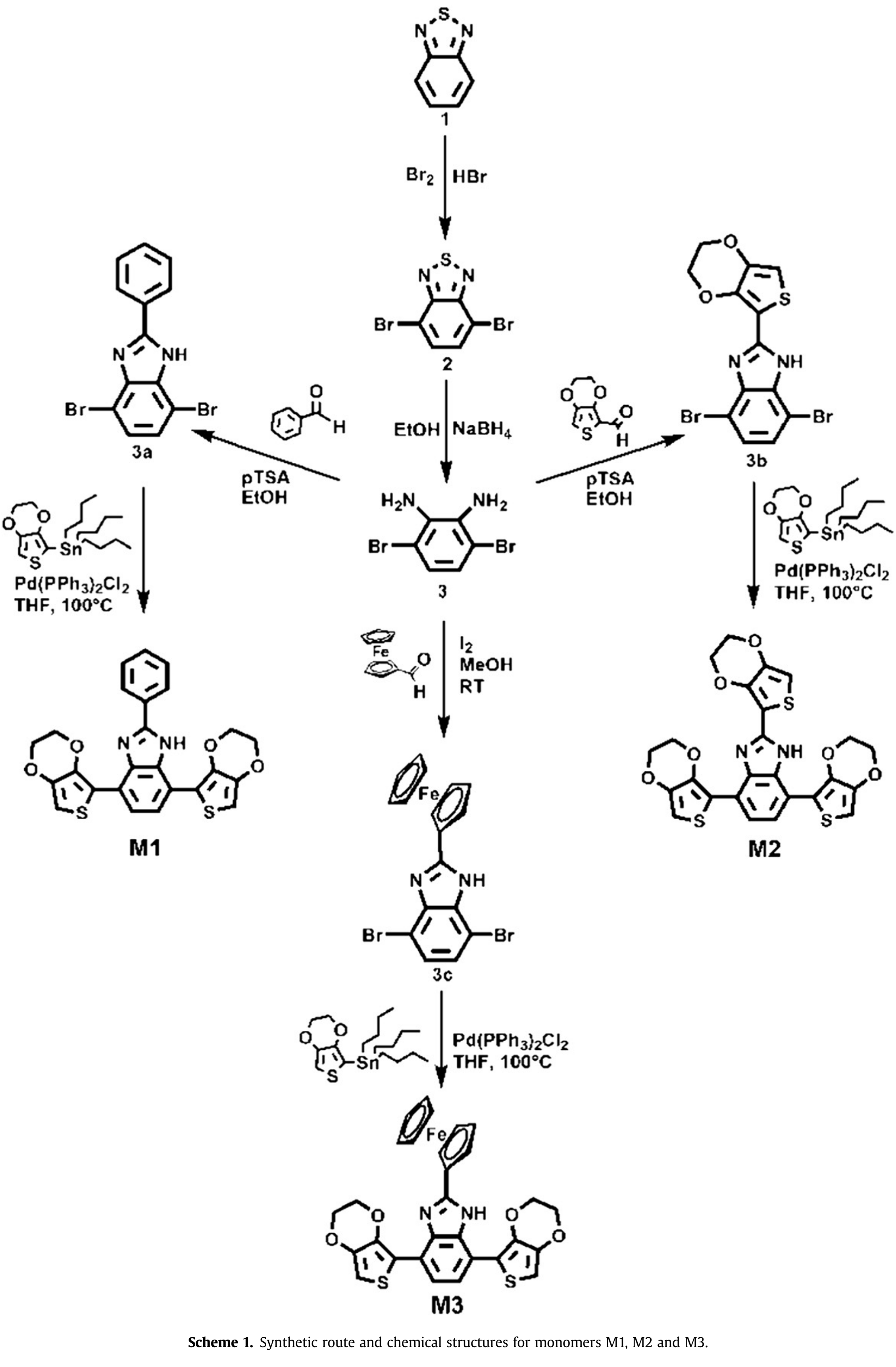

Scheme 1. Synthetic route and chemical structures for monomers M1, M2 and M3.

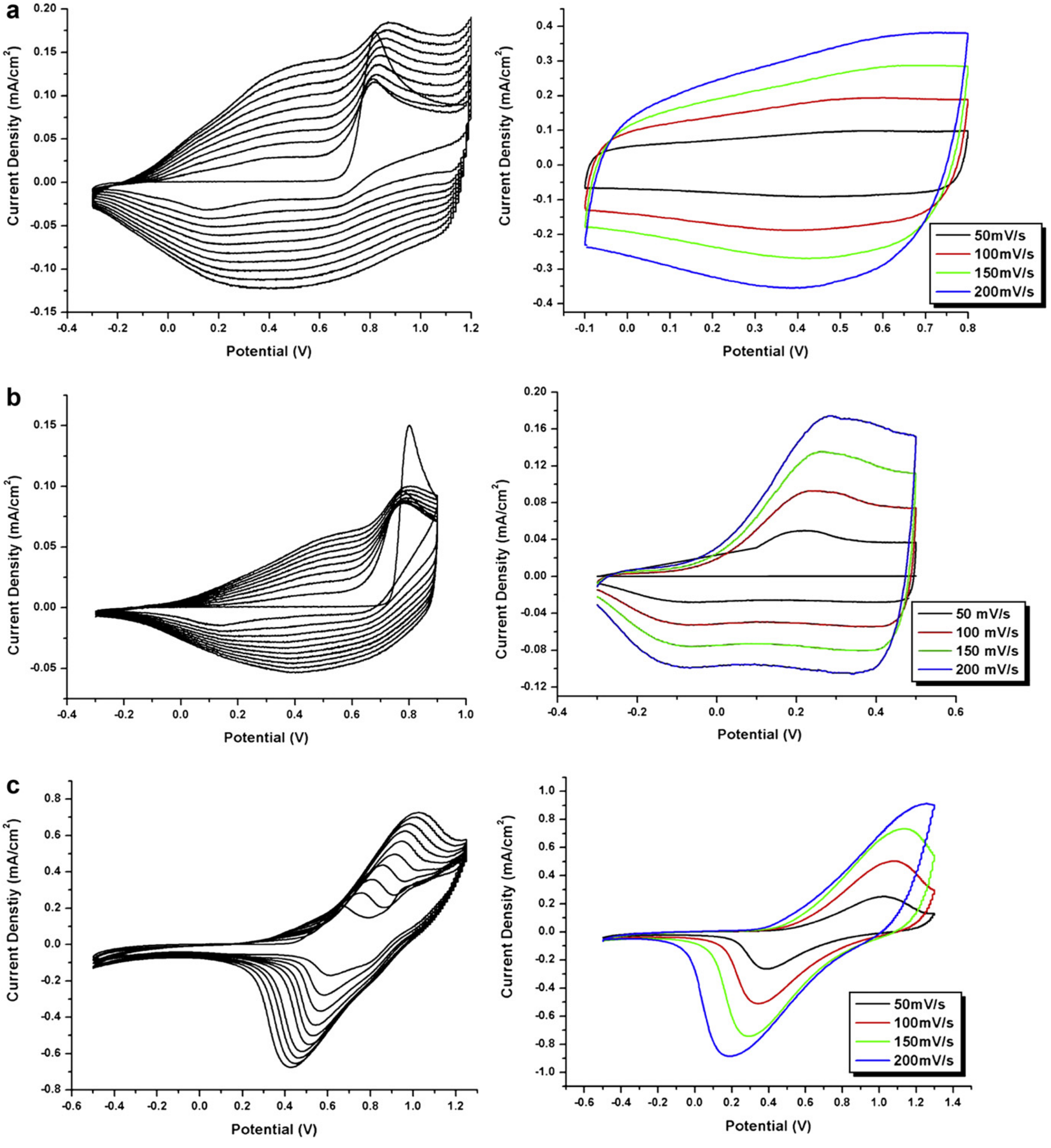

Fig. 1. Electrochemical polymerizations of monomers (left) and scan rate dependence of corresponding polymers (right); a) M1 and P1, b) M2 and P2, and c) M3 and P3.

Subsequent reduction of **2** was achieved using excess amount of $NaBH_4$ in ethanol (EtOH) [19]. In order to observe pendant group effect on optoelectronic properties different aromatic aldehydes were condensed with 3,6-dibromobenzene-1,2-diamine (**3**). Commercially available benzaldehyde and easily synthesized 2,3-dihydrothieno[3,4-*b*][1,4]dioxine-5-carbaldehyde [7] were used in condensation reaction with catalytic amount of p-toluenesulfonic acid (pTSA) in EtOH to give corresponding brominated benzimidazole derivatives 4,7-dibromo-2-phenyl-1*H*-benzo[d]imidazole (**3a**) and 4,7-dibromo-2-(2,3-dihydrothieno[3,4-*b*][1,4]dioxin-5-yl)-1*H*-benzo[d]imidazole (**3b**) [11a]. Ferrocene functionalized benzimidazole (**3c**) was synthesized via different method with a good yield (77%). **3a**, **3b** and **3c** were then coupled with tributyl(2,3-dihydrothieno[3,4-*b*][1,4]dioxin-7-yl)stannane [20] in the presence of Pd $(PPh_3)Cl_2$ as the catalyst in THF to give **M1**, **M2** and **M3**, respectively.

3.2. Electrochemistry

M1, **M2** and **M3** were polymerized potentiodynamically on ITO coated glass slides in a mixture of dichloromethane (DCM) and acetonitrile (ACN) (5/95, v/v) using 0.1 M tetrabutylammonium hexafluorophosphate ($TBAPF_6$) supporting electrolyte with repeated scan intervals −300 mV/1200 mV, −300 mV/900 mV, and −500 mV/1250 mV; respectively (Fig. 1). In the first cycle of voltammograms, irreversible monomer oxidation peaks at 0.82 V (**M1**) and 0.80 V (**M2**) appeared and reversible polymer redox peaks for **P1** were centered at 0.56 V and 0.38 V versus Ag wire pseudo reference electrode. Polymer p-doping/dedoping potentials were decreased for **P2** (0.51 and 0.33 V) as benzene was replaced by electron rich 3,4-ethylenedioxy thiophene (EDOT) unit (Fig. 1). During stepwise oxidation of **M3**, first peak for Fc/Fc^+ oxidation was seen at 0.65 V and the monomer oxidation peak was appeared at 0.96 V. After monomer oxidation, a reduction appeared at 0.6 V. This reduction leads to electrode surface passivation hampering to observe the ferrocene reduction peak. Nonetheless, after repetitive cycles of electropolymerization Fc^+/Fc reduction peak became visible (as overlapped with the polymer reduction peak) since polymer reduction peak shifted to less positive potentials. Big difference between doping/dedoping (1.06/0.40 V) potentials for **P3** confirms a multi-electron redox process due to electroactive and bulky ferrocenyl substituents on BIm units. These bulky groups also affect the insertion of the electrolyte anion to the polymer film and the rate of quinoid to benzenoid transformation.

Among electron accepting benzazoles (BTd, BIm, BTz and BSe), BSe was shown to be the best electron accepting unit. Although it is expected to be the opposite, replacement of sulphur atom by selenium results in a better electron donating character among the donor units (thiophene, selenophene) [21]. Also the electron accepting capacity of BSe is better than that of BTd. This trend can be explained by the large polarizability and the electrochemical amphotericity of selenium atom as stated by Yamamoto [11b] and Suzuki [19]. In addition, the difference between C–X–C and N–X–N bonds may play an important role (X = Se or S) as well. Since all above mentioned acceptor units differ by the atoms at 2-positions (S, Se, C, N), electrochemical properties of the DAD monomers are affected by the polarizability differences between these atoms. In this context, BIm unit would be expected to have electron accepting ability between BTd and BTz since it possesses a C atom. However, since the DAD type polymers are the so called copolymers, donor acceptor match is the point of importance to achieve dual character with enhanced electronic and optical properties. Thus, the comparison should be related to the resulting

Table 1
Chemical structures and optoelectronic properties of polymers containing different benzazoles as the acceptor units.

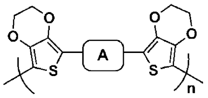

	$E_{m,a}$ (V)	$E_{p,a}$ (V) $E_{p,c}$ (V)	λ_{max} (nm)	Eg (eV)[a]	Colors[b]	Optical Contrasts	Switching Times	Ref.
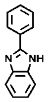	0.82	0.56 0.38	338 580	1.75 (580 nm)	Blue/Transparent Sky Blue	44.5% (580 nm) 75.3% (1800 nm)	0.4 s (580 nm) 0.6 s (1800 nm)	[c]
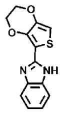	0.80	0.51 0.33	360 560	1.69 (560 nm)	Blue/Transparent Light Gray	44.5% (560 nm) 71.4% (1800 nm)	0.4 s (560 nm) 0.5 s (1800 nm)	[c]
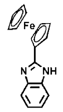	0.96	1.06 0.40	332 513	1.77 (513 nm)	Purple/Blue	10.0% (513 nm) 36.0% (1370 nm)	2.5 s (513 nm) 2.0 s (1800 nm)	[c]
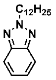	0.97	0.23 −0.04	618	1.60 (618 nm)	Blue/Transparent	53%-618 nm 71%-1600 nm	1.1 s (618 nm)	[15]
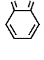	0.95	−0.06 −0.26	428 755	1.19 (755 nm)	Green/Transparent Sky Blue	23%-755 nm 72%-1500 nm	0.4 s (755 nm) ~1.0s (1500 nm)	[13]
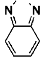	0.85	−0.09 −1.24	343 448 796	1.13 (796 nm)	Green/Transparent Sky Blue	27.3% (448 nm) 10.9% (796 nm)	2.1 s (448 nm) 1.7 s (796 nm)	[14]

[a] Optical band gaps which were calculated from the onset of $\pi-\pi^*$ transitions in UV.
[b] Representing colors for neutral/oxidized states.
[c] This work.

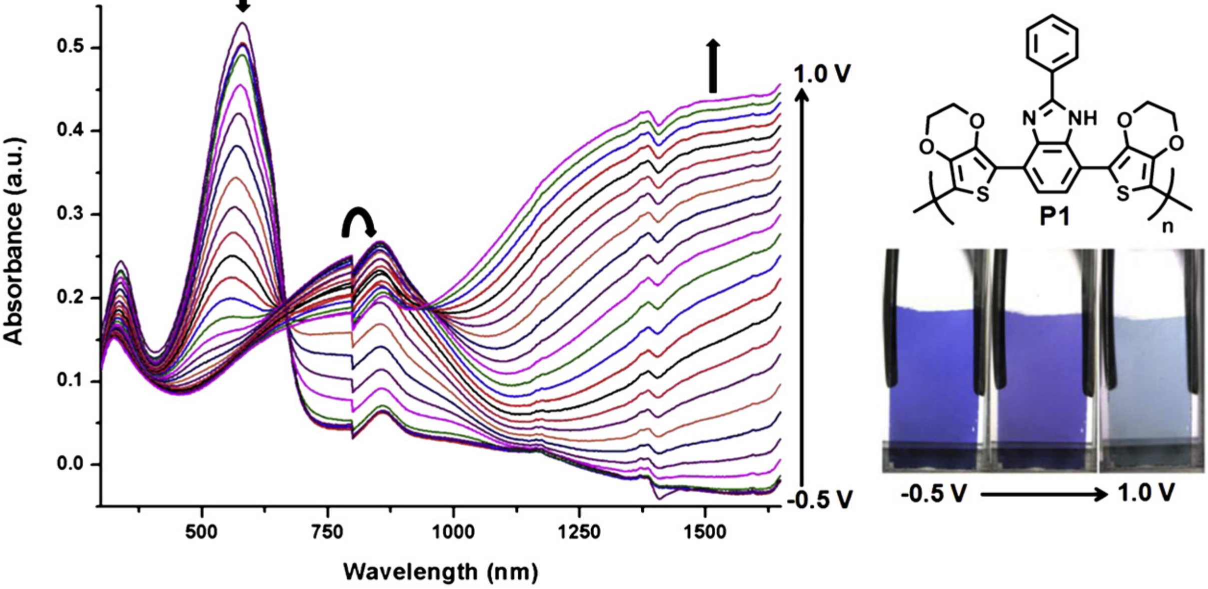

Fig. 2. Electronic absorption spectra of P1 film in 0.1 M TABPF$_6$/ACN solution between −0.5 V and 1.0 V with 0.05 V potential intervals.

DAD polymers rather than the corresponding homo-polymers. In the series of benzazole bearing polymers (Table 1), only BIm based polymers were not n-dopable which confirms a poor match between BIm and EDOT unit in the context of DA approach.

The difference between the oxidation potentials of **M1**, **M2** and **M3** can not be simply explained by the electron density and the electron donating capacity of the subtituents, because all the three substituents are expected to affect the planarity of the imidazole ring differently. Corresponding polymers, **P1**, **P2** and **P3** were subjected to scan rate alternation experiments in order to determine diffusion dependencies of thin films on the working electrodes (ITO). Linear relationships between scan rates and current intensities showed that all polymers were well adhered on ITO surface and the electrochemical processes were not limited by diffusion control [22].

3.3. *Spectroelectrochemistry*

Spectroelectrochemical studies of the polymers were performed in order to examine their optical and structural responses upon doping process which proves the evolution of the charge carries in the structure. UV–vis–NIR spectra for electrochemically coated polymer films acquired during stepwise oxidation in a monomer free, 0.1 M TBAPF$_6$/ACN solution.

Although BIm based polymers exhibited two transitions due to their donor-acceptor nature, the lowest energy transitions affected the colors of neutral films dominantly since other transitions were not in the visible region. The two transitions in DAD type polymers are attributed to the transitions from the thiophene-based valence band to its antibonding counterpart (high-energy transition) and to the substituent-localized conduction band (low-energy transition)

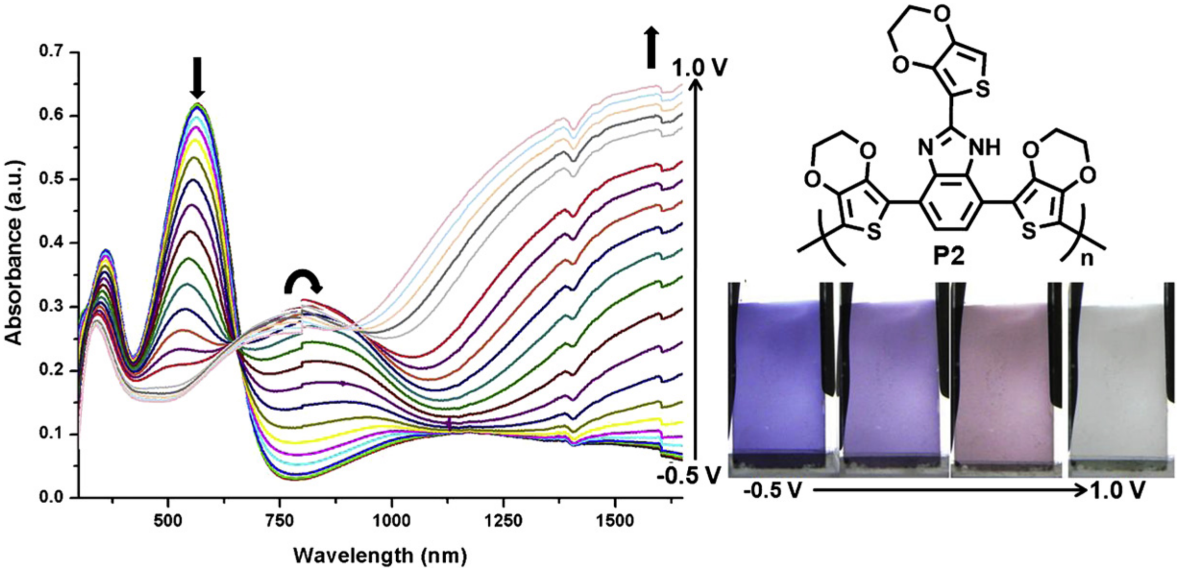

Fig. 3. Electronic absorption spectra of P2 film in 0.1 M TABPF$_6$/ACN solution between −0.5 V and 1.0 V with 0.05 V potential intervals.

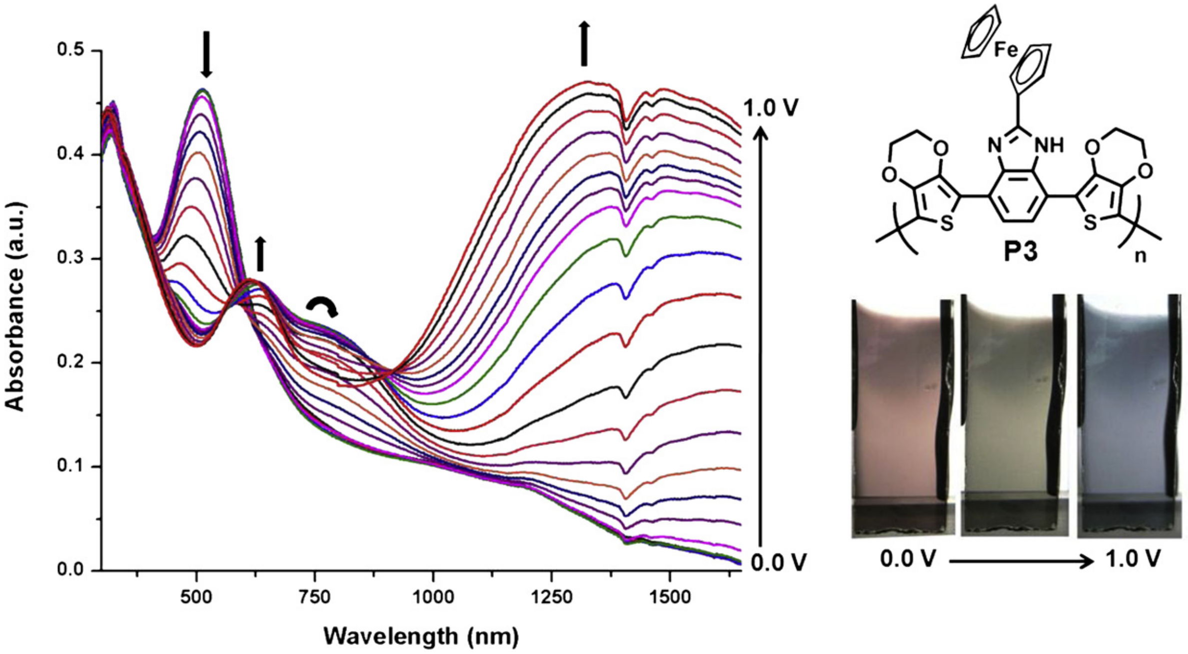

Fig. 4. Electronic absorption spectra of P3 film in 0.1 M $TABPF_6$/ACN solution between 0.0 V and 1.0 V with 0.05 V potential intervals.

hence, interactions between donor and acceptor units (their match) determine the energy and intensity of these transitions. This phenomenon is in agreement with the blue shifts and decreasing intensity for series of polymers with decreasing acceptor strengths.

Neutral state absorption maxima for polymers were recorded as 580 nm for **P1**, 560 nm for **P2** and 513 nm for **P3**. These absorptions were also all blue shifted compared to other benzazole and EDOT based polymers. This can be attributed to the non-decreased band gap due to poor donor acceptor match between EDOT and BIm which was also the case in BTz. However, for polymers with stronger acceptors BTd and BSe have energy transitions at around 400 and 700 nm which resulted in green neutral polymers whereas **P1** and **P2** were blue and **P3** was purple in their neutral states. Optical band gaps of the polymers were calculated as 1.75, 1.69 and 1.77 eV for **P1**, **P2** and **P3** respectively from the onset of $\pi-\pi^*$ transitions in the visible region.

Upon oxidation of polymers (**P1**, **P2** and **P3**), formation of charge carriers such as polarons and bipolarons [23] led to new absorption bands in NIR while absorptions for the neutral states were decreasing. In-situ spectroelectrochemical studies for the polymer films showed that the color of the film changed from saturated blue to highly transmissive sky-blue for **P1**. On the other hand, its EDOT substituted homologue **P2**, revealed different shade and tones as the transition colors since polaronic absorption bands tailed more into the visible region. Although both **P1** and **P2** showed identical polaronic absorptions, these bands decreased less with increasing

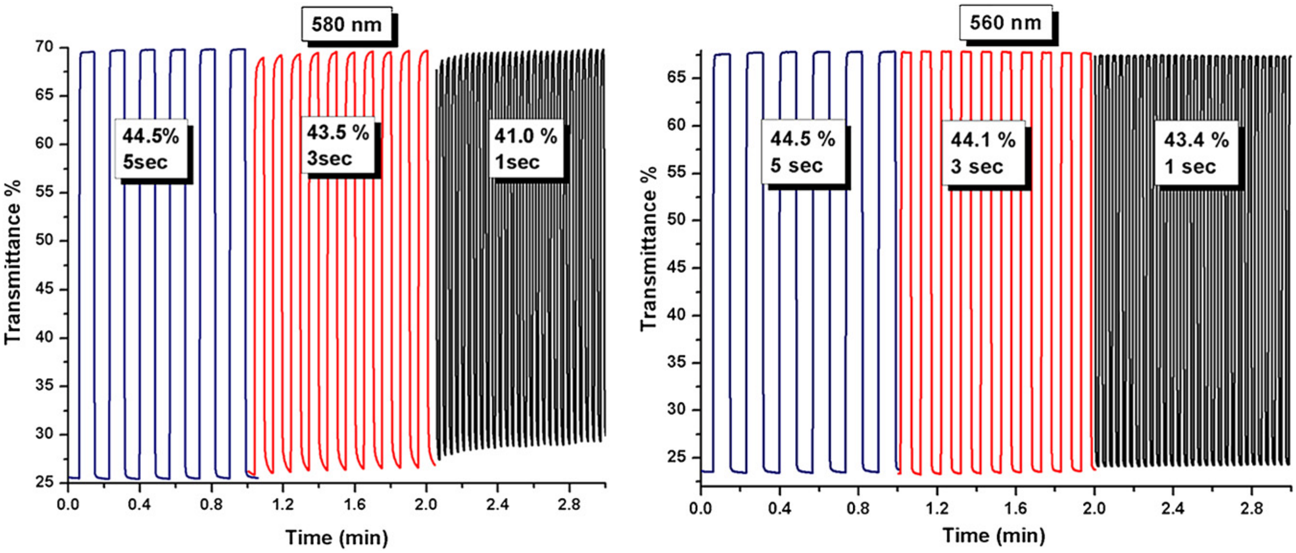

Fig. 5. Square wave potential step chronoapsorptometry studies of P1 and P2 monitored at 580 nm and 560 nm between −0.5 V and 1.0 V (vs. Ag wire). Switching time intervals: 5 s, 3 s and 1 s.

Table 2
Optical contrasts and switching abilities of polymers **P1**, **P2** and **P3**.

	Switching intervals	T_{red}%	T_{ox}%	ΔT%	t_{ox} (s)
P1	5 s	25.2	69.7	44.5	0.42
λ_{max}: 580 nm	3 s	26.0	69.5	43.5	0.60
	1 s	27.9	68.9	41.0	0.40
P1	5 s	17.2	92.5	75.3	0.62
λ_{max}: 1800 nm	3 s	18.5	89.4	70.9	0.60
	1 s	18.8	83.8	65.0	0.52
P2	5 s	23.2	67.9	44.5	0.48
λ_{max}: 560 nm	3 s	23.6	67.7	44.1	0.40
	1 s	24.0	67.4	43.4	0.42
P2	5 s	17.1	88.5	71.4	0.54
λ_{max}: 1800 nm	3 s	17.3	88.4	71.1	0.36
	1 s	17.4	87.6	70.2	0.30
P3	5 s	22.3	32.5	10.2	2.5
λ_{max}: 513 nm					
P3	5 s	41.2	79.4	38.2	2.0
λ_{max}: 1800 nm					

potential for **P2** than those of **P1** due to simultaneous formation of polaronic and bipolaronic charge carriers (Figs. 2 and 3). Additionally, isosbestic point at around 650 nm for **P2** confirmed the coexistence of more than one charged species absorbing in the visible region on the polymer chain. These different species contribute differently to the resulting color of the film in the sense that as if one mixes two different colored polymers [24]. As their absorption bands react differently upon stepwise oxidation, multicolored states are achieved. It can also be generalized that polymers having isosbestic points usually result in multicolored achievable states [25].

Color of **P3** in its different redox states were affected by the bulky and visible absorber Fc pendant group. Oxidation of **P3** film resulted in a similar behavior to **P1** and **P2** at its early doping stages, but later a new absorption band was emerged at 625 nm which stands for polaronic absorption bands (770 nm) with increasing bias due to characteristic blue color of Fc^+ ions. This visible absorption of Fc^+ groups conduced with a blue colored oxidized state for **P3** film. Moreover, partial oxidation of **P3** allowed detection of a gray colored transition state as a consequence of mixing different colored states of main chain and Fc groups (Fig. 4).

3.4. *Kinetic studies*

Optical contrasts were monitored as the function of time at the maximum absorption of **P1** and **P2** in order to characterize their response times and switching abilities. Electrochemically polymerized films were subjected to chronoabsorptometry studies in a monomer free solution containing 0.1 M $TBAPF_6$/ACN. As depicted in Fig. 5, both polymers **P1** and **P2** revealed optical contrast values of ca. 45% at their short wavelength maximum absorptions at 580 nm and 560 nm. Although for **P1** a variation in electrochromic contrast of 4% was observed as the stepping interval was changed from 5 to 1 s, the latter (**P2**) revealed the robustness and the stability of the material applications like electrochromic devices and optical displays. Table 2 summarizes the switching abilities for **P1** and **P2** at their dominant wavelengths in visible and NIR regions. As seen, it does not matter how fast the polymer films were switched, the time required to switch between their neutral and oxidized states did not change significantly which also can be an evidence for the durability of the polymer films.

P2 did not exhibit a difference in its optical contrast values ($44.5\% \geq 43.4\%$) even though the switching time was changed to 1 s. 75.3% and 71.4% optical contrast values were determined for **P1** and **P2** at 1800 nm which are quite impressive and eminent to use these materials can be used in NIR applications [26] (Fig. 6). Among others, when switched between its neutral and oxidized states, **P3** showed trapezoidal pulses which resulted in longer switching times (2.5 s) and lower contrast values (10% at 513 nm). This property may stem from the difficulties in charge accumulation due to large differences between polymer chains [27].

Coloration efficiency (CE (η)) is defined as the relationship between the injected/ejected charge density (Qd) and the change in optical density (difference between colored and bleached states), ΔOD, at a specific dominant wavelength (λ_{max}). The desired material or device should exhibit a large optical contrast giving rise to large CEs. Using the related formula, coloration efficiencies for **P1** and **P2** were calculated as 352 cm^2/C and 325 cm^2/C, respectively. Coloration efficiency results for **P3** were not calculated since transmissive (bleached) color in its oxidized form was not achieved.

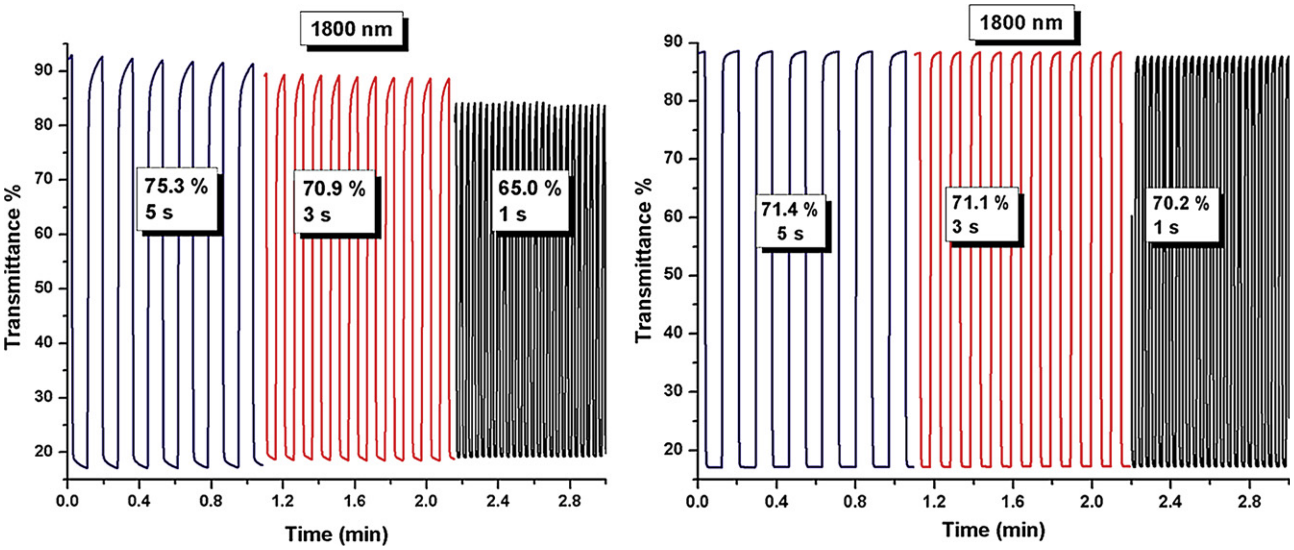

Fig. 6. Square wave potential step chronoapsorptometry studies of P1 and P2 monitored at 1800 nm between −0.5 V and 1.0 V (vs. Ag wire reference electrode). Switch intervals: 5 s, 3 s and 1 s.

4. Conclusion

Three DAD type monomers bearing electron deficient BIm units as the acceptor and electron rich EDOT units as the donor groups were synthesized. Their electrochemically synthesized polymers on ITO coated glass slides were characterized in terms of their electrochemical and optical properties. Electrochemical studies showed that donor acceptor match between BIm and EDOT units is not strong as was the case in the other benzazole bearing DAD type polymers. However, spectroelectrochemical results proved their great candidacy for electrochromic display device applications. Altering the pendant group affected the electrochromic behavior of the resulting polymers dramatically. EDOT substitution on 2-C position of the BIm unit revealed a polymer with multicolored oxidation states within a low potential range whereas phenyl substituted polymer switched between the different shades of the same color. Ferrocene group was also incorporated into polymer chain as a pendant group and its states also contributed to the colors of the polymer. Additionally ferrocene substitution might improve polymers' potential use for biochemical applications which will be investigated in due course. Reported results for all polymers prove the potential use of BIm as an acceptor unit in DAD type polymers. The synthesis of different DAD analogues with different donor units to achieve better donor acceptor match will be the subject of further studies.

Acknowledgement

The authors thank TUBA for financial support.

References

[1] (a) Gunes S, Neugebauer H, Sariciftci NS. Chem Rev 2007;107(4):1324–38;
(b) Bijleveld JC, Zoombelt AP, Mathijssen SGJ, Wienk MM, Turbiez M, de Leeuw DM, et al. J Am Chem Soc 2009;131(46):16616–7;
(c) Park SH, Roy A, Beaupre S, Cho S, Coates N, Moses JSMD, et al. Nat Photon 2009;3:297–302;
(d) Zoombelt AP, Fonrodona M, Wienk MM, Sieval AB, Hummelen JC, Janssen RA. J Org Lett 2009;11(4):903–6;
(e) Baran D, Balan A, Celebi S, Esteban BM, Neugebauer H, Sariciftci NS, et al. Chem Mater 2010;22(9):2978–87;
(f) Li W, Qin R, Zhou Y, Andersson M, Li F, Zhang C, et al. Polymer 2010;51(14):3031–8.

[2] (a) Allard S, Forster M, Souharce B, Thiem H, Scherf U. Angew Chem Int Ed 2008;47(22):4070–98;
(b) McCulloch I, Heeney M, Bailey C, Genevicius K, MacDonald I, Shkunov M, et al. Nat Mater 2006;5(4):328–33;
(c) Chua LL, Zaumseil J, Chang JF, Ou ECW, Ho PKH, Sirringhaus H, et al. Nature 2005;434(7030):194–9;
(d) Leenen MAM, Cucinotta F, Pisula W, Steiger J, Anselmann R, Thiem H, et al. Polymer 2010;51(14):3099–107.

[3] (a) Grimsdale AC, Chan KL, Martin RE, Jokisz PG, Holmes AB. Chem Rev 2009;109(3):897–1091;
(b) Beaupré S, Boudreault PT, Leclerc M. Adv Mater 2010;22(8):E6–27;
(c) Kamtekar KT, Vaughan HL, Lyons BP, Monkman AP, Pandya SU, Bryce MR. Macromolecules 2010;43(10):4481–8.

[4] (a) Invernale MA, Ding Y, Mamangun DMD, Yavuz MS, Sotzing GA. Adv Mater 2010;22(12):1379–82;
(b) Dyer AL, Craig MR, Babiarz JE, Kiyak K, Reynolds JR. Macromolecules 2010;43(10):4460–7;
(c) Sharmoukh W, Ko KC, Ko JH, Jung G, Noh C, Lee JY, et al. Org Lett 2010;12(14):3226–9;
(d) Ding Y, Invernale MA, Sotzing GA. ACS Appl Mater Interfaces 2010;2(6):1588–93;
(e) Beaujuge PM, Ellinger S, Reynolds JR. Nat Mater; 2008:795–9;
(f) Invernale MA, Bokria JG, Ombaba M, Lee KR, Mamangun DMD, Sotzing GA. Polymer 2010;51(2):378–82.

[5] Argun AA, Aubert PH, Thompson BC, Schwendeman I, Gaupp CL, Hwang J, et al. Chem Mater 2004;16(23):4401–12.

[6] Beaujuge PM, Reynolds JR. Chem Rev 2010;110(1):268–320.

[7] Thompson BC, Kim YG, McCarley TD, Reynolds JR. J Am Chem Soc 2006;128(39):12714–25.

[8] Mullekom HAM, Vekemans JAJM, Havinga EE, Meijer EW. Mater Sci Eng 2001;R32:1–40.

[9] Thomas CA, Zong K, Abboud KA, Steel PJ, Reynolds JR. J Am Chem Soc 2004;126(50):16440–50.

[10] Salzner U, Köse ME. J Phys Chem B 2002;106(10):9221–6.

[11] (a) Yamamoto T, Sugiyama K, Kanbara T, Hayashi H, Etori H. Macromol Chem Phys 1998;199(9):1807–13;
(b) Kanbara T, Yamamoto T. Chem Lett 1993;22(3):419–22;
(c) Tanimoto A, Yamamoto T. Macromolecules 2006;39(10):3546–52;
(d) Tanimoto A, Yamamoto T. Adv Synth Catal 2004;346(13):1818–23;
(e) Yasuda T, Imase T, Yamamoto T. Macromolecules 2005;38(17):7378–85;
(f) Yamamoto T. Bull Chem Soc Jpn 2010;83(5):431–55.

[12] Blanchard P, Raimundo JM, Roncali J. Synth Met 2001;119(1–3):527–8.

[13] Durmus A, Gunbas GE, Camurlu P, Toppare L. Chem Commun; 2007:3246–8.

[14] Cihaner A, Algı F. Adv Funct Mater 2008;18(22):3583–9.

[15] Balan A, Gunbas G, Durmus A, Toppare L. Chem Mater 2008;20(24):7510–3.

[16] (a) Barker HA, Smyth RD, Weissbach H, Toohey JI, Ladd JN, Volcanic BEJ. Biol Chem 1960;235(2):480;
(b) Kukalenko SS, Bovykin BA, Shestakova SI, Omel'chenko AM. Russ Chem Rev 1985;54(7):676.

[17] Ragno G, Risoli A, Ioele G, de Luca M. Chem Pharm Bull 2006;54(6):802–6.

[18] Da Silveria Neto AB, SanťAna AL, Ebeling G, Goncalves SR, Costa EVU, Quina HF. Dupont J Tetrahedron 2005;61(46):10975–82.

[19] Tsubata Y, Suzuki T, Miyashi T, Yamashita Y. J Org Chem 1992;57(25):6749–55.

[20] Zhu SS, Swager TM. J Am Chem Soc 1997;119(51):12568–77.

[21] Xu J, Hou J, Zhang S, Nie G, Pu S, Shen L, et al. J Electroanal Chem 2005;578(2):345–55.

[22] Sonmez G, Schwendeman I, Schottland P, Zong K, Reynolds JR. Macromolecules 2003;36(3):639–47.

[23] Bredas JL, Chance RR, Silbey R. Phys Rev B 1982;26(10):843–54.

[24] Sönmez G. Chem Commun; 2005:5251–9.

[25] Balan A, Baran D, Gunbas G, Durmus A, Ozyurt F, Toppare L. Chem Commun; 2009:6768–70.

[26] (a) McDonagh AM, Bayly SR, Riley DJ, Ward MD, McCleverty JA, Cowin MA, et al. Chem Mater 2000;12(9):2523–4;
(b) Meng H, Tucker D, Chaffins S, Chen Y, Helgeson R, Dunn B, et al. Adv Mater 2003;15(2):146–9.

[27] Li M, Sheynin Y, Patra A, Bendikov M. Chem Mater 2009;21(12):2482–8.